Measurement of Charge Density in Methane Fired Diffusion and Premixed Flames Using Electrostatic Probes

Yong Yan, *Fellow, IEEE*, Jiali Wu, *Graduate Student Member, IEEE* and Yonghui Hu, *Senior Member, IEEE*

***Abstract*—The charge density in a flame contains important information about the combustion processes that is difficult to obtain due to fast, complex, and highly exothermic reactions. This paper presents a study of using electrostatic probes to measure the charge density in methane fired diffusion and premixed flames. The sensing principle, practical design, and performance assessment of the electrostatic probe are presented. Comparative experimental studies with a reference ion-current sensor carried out on a combustion test rig indicate that the fluctuation of the signal from the electrostatic probe arises from the variation in the charge density in a flame. A dimensionless index, combining the average of local peak values in the electrostatic signal with the flame oscillation frequency, is adopted as an indicator of the charge density. Experimental results demonstrate that the charge density in a methane diffusion flame has an increasing trend with the fuel flowrate varying from 0.80 L/min to 1.20 L/min. The charge density in a methane-air premixed flame yields a decreasing trend with the equivalence ratio ranging from 0.54 to 0.75, then increases and reaches a local peak at the equivalence ratio of 1.03, and continues to increase when the equivalence ratio varies from 1.03 to 3.50. The charge density in the inner cone is higher than that in the outer cone for diffusion and premixed flames. The results obtained suggest that the developed electrostatic probe and the index can be used to indicate the charge density in diffusion and premixed flames.**

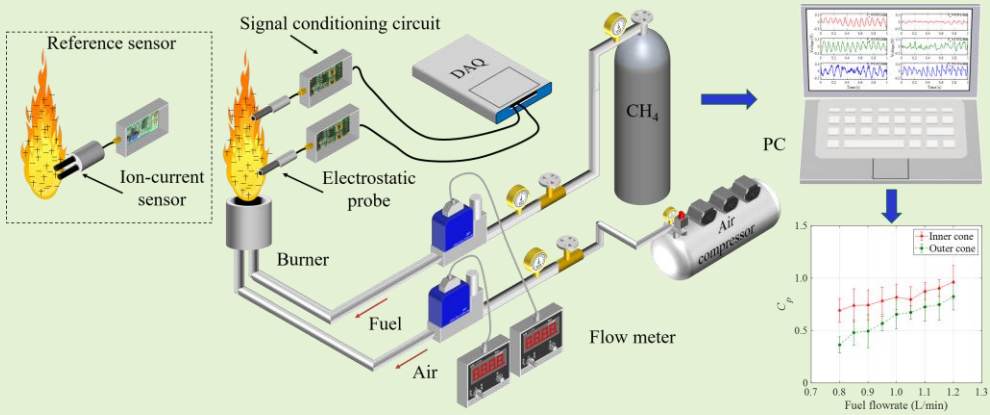

***Index Terms*—Flame, charge density, electrostatic probe, combustion monitoring.**

I. Introduction

THE analysis of combustion processes is difficult since fast, complex, and highly exothermic reactions are involved. In general, high pressures and multiple interferences such as dust and particles as well as background radiation are present in the transient reactions, posing the challenge for the monitoring and characterization of a flame. Earlier studies of burner flames [1-4] are concerned mostly with optical and thermoacoustic properties of flames and little on their electrical properties. Chemical reactions in a flame produce charged species such as free electrons, ions, and soot particles [5-8]. The charge density and its spatial distribution in a flame are directly related to the chemical reactions, containing important information on the combustion processes [9]. Therefore, measurement of charge density in a flame is desirable to gain a good understanding of the reaction and combustion processes.

An active negatively biased probe, which adopts the burner as the reference electrode, has been widely employed to detect the ion current to determine the ion concentration and its distribution in a flame [9, 10]. Another kind of active sensing probe adopts a platinum wire as the detecting part and a supporting tube as the reference electrode [11]. The displacement speed of the chemical reaction zone in a furnace can be obtained by cross-correlation analysis of the ion-current signals from two identical probes [11]. Peerlings *et al.* [12] employed the generation rate of ions as an indicator of the dynamic flame response. Power spectral analysis of the

The authors wish to acknowledge the National Natural Science Foundation of China (No. 61673170 and No. 51827808) for providing financial support for this research. The IEEE Instrumentation and Measurement Society is acknowledged for offering an IEEE Graduate Fellowship Award in relation to the research reported in this paper. (Corresponding author: Jiali Wu.)

Y. Yan is with School of Control and Computer Engineering, North China Electric Power University, Beijing 102206, China (visiting professor) and with School of Engineering, University of Kent, Canterbury, Kent CT2 7NT, U.K. (e-mail: y.yan@kent.ac.uk).

J. Wu and Y. Hu are with School of Control and Computer Engineering, North China Electric Power University, Beijing 102206, China (e-mail: jlwu@ncepu.edu.cn, huyhui@gmail.com).

current signal from an ion-current sensor was conducted to obtain the oscillation frequency of a premixed flame [13] and detect lean blowout in a pulse combustor [14]. Although such ion-current sensors provide localised information about a flame, the external voltage applied to the flame can affect the combustion rate, and the shape, stability of the flame.

Mass spectrometers were employed to identify the positive and negative ions, particularly in hydrocarbon flames [15-17]. Guo *et al.* [15] collected the total flux of cations that collides with a conductive plate perpendicular to the flame axis and detected a saturation current to measure the concentration of positive ions in a flat flame. Hayhurst *et al.* [16] investigated the effect of applied electric fields on the mass spectrometric sampling of positive and negative ions from a flat flame. In these cases, the flame is generally doped with an appropriate additive (the easily-ionizable alkali metal) to allow the degree of ionization to be enhanced above the natural ionization level. Mass spectrometers provide accurate and easily reproducible results. However, such instruments have some problems including the flow field of the flame possibly being disturbed, chemical reactions catalysed by the material of the sampling nozzle and the influences of applied electric fields on the motion of ions from a flame into the sampling system [17].

There has been limited research on the measurement of charge density in burner flames using passive electrostatic probes so far. This paper introduces the sensing principle, practical design and performance assessment of electrostatic probes. Electrostatic probes extended into the flame can detect the charges of positive and negative ions, free electrons together with charged soot particles in the flame. Passive electrostatic probes have no requirement for an external electric field, which is advantageous over ion-current sensors. In comparison with mass spectrometers, electrostatic probes have the advantages of simplicity in sensor structure and cost-effectiveness, making the technique suitable for applications to a wider range of industrial processes. Electrostatic probes can be used to measure the charge density for any flames in industrial furnaces for power generation, metal smelting etc [11]. Electrostatic probes may also be used in some combustion systems such as internal combustion engines [14]. An isolated electrostatic probe is used in this study. The isolated electrostatic probe detects the amount of induced charge through electrostatic sensing, but may lose partial information about transferred charge. However, the isolated electrode in an electrostatic probe has no direct contact with the charged species in the flame and thus yellow tungsten trioxide, a kind of N-type semiconductor material that may affect the electrical conductivity of the tungsten electrode, will not be produced on the electrode surface [18]. Experimental investigations into the measurement of charge density in methane fired diffusion and premixed flames using electrostatic probes are conducted on a combustion rig.

II. Measurement Method and Sensor Design

A. Sensing principle

Although a flame contains charged species such as free electrons, positive and negative ions together with charged soot particles, it is weak plasma and electrically neutral as an integral whole [16]. The induced signal from the isolated electrode placed around the flame is entirely due to electrostatic induction from the charged species and thus its amplitude is very small and negligible. The signal from the exposed electrode installed around the flame originates from charge transfer and its amplitude is mainly related to the distance from the flame boundary to the electrode [19]. Information about the density of charged species in the flame can only be acquired using an isolated electrostatic probe inserted into the flame.

Fig. 1 shows the sensing principle of the electrostatic probe for the measurement of charge density in a burner flame. The isolated electrode of the probe inserted into the flame provides the sensing volume, i.e. electrostatic induction takes place through the insulated coating of the electrode. The installation location of the probe can be adjusted to measure the interested zones of the flame. A large number of charges are continuously generated and distributed in the flame. If the density of charged species did not change at all and its distribution was uniform, the induced charge on the electrostatic probe arising purely from electrostatic induction would keep constant and there would be no current flowing through the electrode. In practice, the density and spatial distribution of charged species in the flame vary with time due to the complex chemical reaction, giving rise to the fluctuation of the spatial charge density in the vicinity of the probe and hence the amount of induced charge on the isolated electrode of the probe. The induced charge on the electrostatic probe arises from a combination of free electrons, positive and negative ions together with charged soot particles in the flame. Although charge neutralization may occur, the concentrations of positive and negative elements generated in the flame are not equal. The amount of induced charge indicates the overall density of charged species in the flame. The induced charge representing the density of charged species can be converted into a voltage signal using a current-to-voltage converter. The voltage signal is further amplified with a secondary amplifier and denoised with a low-pass filter. In addition, the overall polarity of charged species can be determined from the polarity of the induced-charge signal from the electrostatic probe.

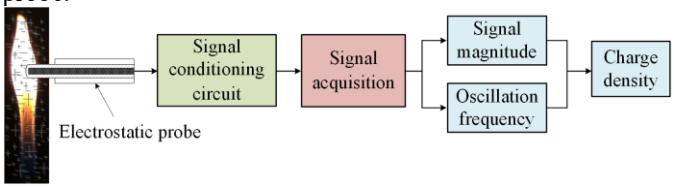

Fig. 1. Sensing principle of the electrostatic probe for the measurement of charge density in a burner flame.

B. Measurement method

The magnitude of the induced charge signal is directly related to the charge density in the flame. The time-domain parameters of the charge signal, including the average of local peak values (V_p), root mean square (rms) value (V_{rms}) and energy (E) of the signal, are useful indicators of the signal magnitude. There are several local peaks that should be identified in the charge signal. A point in the signal is regarded as a local peak if its amplitude is between two consecutive local minima. The average of local peak values is given by:

$$\overline{V_p} = \frac{1}{n}\sum_{i=1}^{n} V_p(i) \tag{1}$$

where $V_p(i)$ is the i-th local peak value, n is the number of local peak values. V_{rms} is determined from:

$$V_{rms} = \left(\frac{1}{N}\sum_{j=1}^{N} v_j^{\,2}\right)^{\frac{1}{2}} \tag{2}$$

where v_j (j = 1, 2, …, N) denotes the discrete-time sampled signal, N is the number of samples in the discrete-time signal. The energy of the signal is expressed as:

$$E = \sum_{j=1}^{N} v_j^{\,2} \tag{3}$$

The amount of induced charge on the electrostatic probe is dependent on a wide range of factors, making it difficult to obtain absolute charge density in the flame [3]. The signal magnitude is nondimensionalized according to the following equation to characterize the relative magnitude of the charge density in the flame under various operating conditions:

$$S_{k,\mathrm{nond}} = \frac{S_k}{S_{k,\max}} \tag{4}$$

where S_k represents the signal magnitude, $k = p$, rms or E, and S_p, S_{rms}, S_E stand for the average of local peak values, rms value and energy of the signal, respectively. $S_{p,max}$ and $S_{rms,max}$ denote the highest value in the sampled signal, and $S_{E,max}$ the square of the highest value in the signal.

Suppose the variation in the induced charge is approximated using a sinusoidal function $Q = A \sin(2\pi f t)$, where A denotes the amplitude and f the oscillation frequency. The signal from the electrostatic probe, i.e. the induced-current signal, is the time derivative of the induced-charge signal. The induced-current signal is expressed as $I = 2\pi A f \cos(2\pi f t)$. The magnitude of the induced-current signal is proportional to the magnitude and oscillation frequency of the induced-charge signal [20]. To take the influence of the oscillation frequency on the magnitude of the induced-current signal into consideration, the index charge density (C), which divides the dimensionless signal magnitude by the oscillation frequency, is introduced to acquire a more accurate characterization of the charge density in the flame, i.e.

$$C_k = \frac{S_{k,\mathrm{nond}}}{F_{\mathrm{nond}}} \tag{5}$$

where C_p, C_{rms}, C_E stand for the charge density characterized using the average of local peak values, rms value and energy of the electrostatic signal, respectively. F_{nond} is the dimensionless oscillation frequency. The dimensionless oscillation frequency F_{nond} is given by:

$$F_{\mathrm{nond}} = \frac{F}{f_{\mathrm{sec}}} \tag{6}$$

where F is the oscillation frequency obtained from power spectral analysis of the electrostatic signal. Previous studies [21] indicate that a diffusion flame has a single dominant frequency component, whereas a premixed flame contains a wide range of frequencies. The frequency corresponding to the largest peak in the power spectrum is regarded as the measured oscillation frequency of the diffusion flame. The oscillation frequency of the premixed flame takes the contributions of all components over the entire frequency spectrum into consideration [21]. The discussions about the flame oscillation frequency obtained using the developed electrostatic probe will be presented in Section III. C 2). f_{sec} denotes the frequency corresponding to the 2-rd order harmonics in the power spectrum.

C. Sensor design

The structure of the isolated electrostatic probe is illustrated in Fig. 2. The probe is composed of a tungsten electrode, a quartz insulating tube and a grounded supporting tube. The electrode is supported with the hollow stainless-steel tube with an outer diameter of 4 mm, and the quartz insulating tube with a round tip provides insulation between the electrode and the stainless-steel tube. The outer diameter of the insulating tube is 3 mm. The diameter of the electrode is 1 mm whilst the electrode protrudes for 10 mm from the end of the stainless-steel tube. The maximum temperature of the flame in the burner is about 1000℃, whereas the common working temperatures of the tungsten electrode and quartz insulating tube are 2000℃ and 1200℃, respectively, which meet the requirement of a sensor for flame monitoring in a high-temperature environment. For the monitoring of a flame with a higher temperature in an industrial furnace, a ceramic or alundum tube may be used as insulation material since their working temperature can reach 1600℃ or higher.

The difference between the isolated and exposed electrostatic probes is that the exposed electrode has no quartz insulating tube so it has direct contact with the flame. Observations of experimental tests on exposed electrostatic probes have shown that, when the exposed tungsten electrode is inserted into the flame, yellow tungsten trioxide WO_3, will be produced on the surface of the tungsten electrode after a few seconds. WO_3 is a kind of N-type semiconductor that may affect the electrical conductivity of the tungsten electrode. From this point of view, the isolated electrostatic probe is adopted in this study.

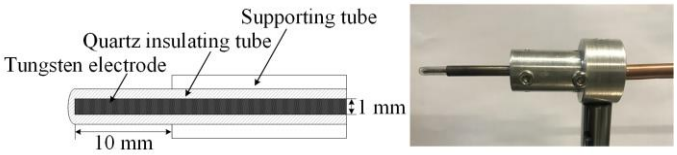

(a) (b)

Fig. 2. Electrostatic probe. (a) Design and structure of the electrostatic probe. (b) Photo of the electrostatic probe.

Fig. 3 shows the signal conditioning circuit mounted on the side of printed circuit board, which is enclosed within a grounded metal box to avoid external electromagnetic interference. The circuit connects to the probe via shielded coaxial cables and BNC (Bayonet Neill–Concelman) connectors. The circuit board is powered by a ±2.5 V dual power supply. A standard MINI USB connector with compact, simple and reliable structure is used for power and signal transmission.

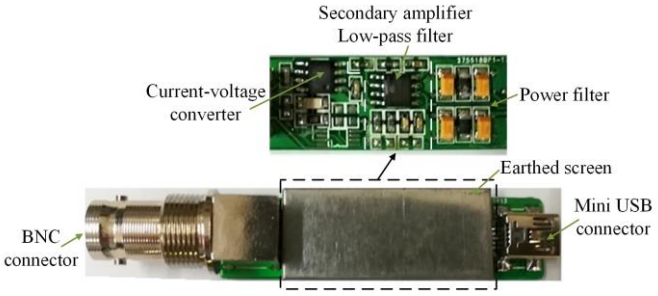

Fig. 3. Signal conditioning circuit.

III. Experimental Setup

A. Test rig

The combustion rig used for performance assessment of the developed electrostatic probe is shown in Fig. 4. It consists of a combustion chamber, a burner, two flowmeters for air and fuel, two electrostatic probes, a reference ion-current sensor, a data acquisition system, and a host computer. The length of the rectangular combustion chamber is 80 cm and the height is 70 cm. The combustible mixture flows from the burner outlet with a diameter of 24 mm in the chamber and then is ignited, generating cone-shaped flames. The flame structure (shape and length) depends on the mixing pattern of the air and the fuel. According to whether the fuel and oxidizer are mixed prior to reacting, the flame can be divided into premixed and diffusion flames. Fig. 5 depicts the structure of typical premixed and diffusion gaseous flames. In a premixed flame, the fuel and the oxidizer are mixed before reacting. In a diffusion flame, however, fuel is supplied to the burner while the oxidizer is supplied from the ambient air, and the mixing and combustion reactions take place together. Both the premixed and diffusion flames have a darker inner cone and a lighter outer cone [22]. The difference is that the premixed flame has a very narrow reaction zone whereas the diffusion flame has a wider region and thus a larger length. Both the inner and outer cones within the flame are of primary interest, two electrostatic probes are thus used to monitor these two cones. The electrostatic probe inserted into the flame is perpendicular to the flame axis. The presence of the electrostatic probe in the flame field may cause some disturbance to the flame itself. In this study, the ratio of the cross-sectional area of the probe (product of the diameter and the length of the probe inserted into the flame) to the cross-sectional area of the flame horizontally across the flame is less than 6.5%, diminishing the effect of the probe on the flame. A National Instruments USB-6363 data acquisition (DAQ) card was used to acquire the signal from the electrostatic probe at a rate of 1 kHz. The electrostatic signal was then transmitted into the host computer and processed.

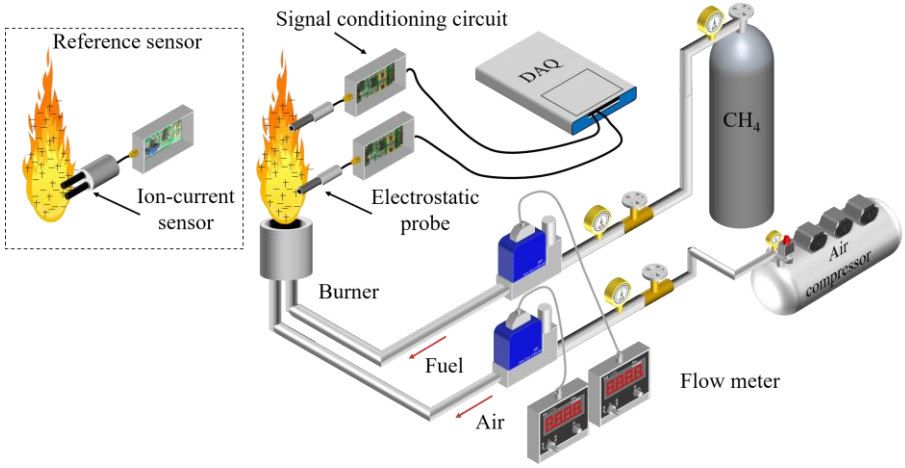

Fig. 4. Constituent elements of the test rig for charge density measurement.

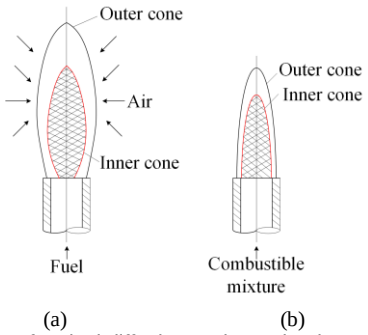

Fig. 5. Structure of typical diffusion and premixed gaseous flames [21]. (a) Diffusion flame. (b) Premixed flame.

Ion-current sensors have been widely used to measure the ion concentration in a flame [12-14]. Before the measurement of charge density in a burner flame, the performance of the electrostatic probe was validated against an ion-current sensor. The ion-current sensor was installed at the inner cone of the flame, which is considered as the primary reaction region of the combustion process in terms of energy conversion and emission formation [23]. The installation height of the ion-current sensor is consistent with that of the electrostatic probe located in the inner cone. The ion current was sampled at a rate of 1 kHz using the data acquisition card to remain consistent with the sampling frequency of the signal from the probe. Assuming the resistance of the fluid medium between the two electrodes was R, the ion current flowing through the two electrodes could be acquired by dividing the applied voltage by the resistance [11]. A conditioning circuit for the ion-current signal, consisting of an DC bridge-based resistor-to-voltage convertor, was built.

B. Test conditions

Experiments were conducted under 29 test conditions, as summarized in Table I. During the experiments, different diffusion flames were produced by adjusting the fuel flowrate F_m with air supplied from the ambient. The fuel flowrate was varied over the range of 0.80 L/min to 1.20 L/min with a step change of 0.05 L/min to achieve various operating conditions. Equivalence ratio Φ is an indicator of the operating condition for a premixed flame since the equivalence ratio is closely related to flame stability, pollutant emissions and heat loss [24]. The equivalence ratio, Φ, is defined as:

$$\Phi = \frac{(\text{fuel-to-air ratio})_{\text{actual}}}{(\text{fuel-to-air ratio})_{\text{stoichiometric}}} \quad (7)$$

where the stoichiometric fuel-to-air ratio is the chemically correct fuel-to-air ratio required for complete combustion of the fuel. For methane, the stoichiometric fuel-to-air ratio is about 1:9.52 by volume. Different premixed flames were created by adjusting the air flowrate at a fixed fuel flowrate of 1.00 L/min. The air flowrate was varied over the range from 2.70 L/min to 17.60 L/min to achieve various equivalence ratios from 0.54 to 1.70 with an increment of 0.07 and from 2.00 to 3.50 with an interval of 0.50.

TABLE I
TEST PROGRAM

Flame type	Fuel flowrate (L/min)	Air flowrate (L/min)	Equivalence ratio
Diffusion flame	0.80-1.20	/	/
Premixed flame	1.00	2.70-17.60	0.54-3.50

The installation location of the electrostatic probe may affect the measurement results as the electrostatic signal is a local measurement. Previous studies indicate that for the inner cone of a methane-fired flame, the temperature at a position above 70% of its length is higher and changes little [25]. For the outer cone, the temperature at 40% and 70% of its length reaches maximum and varies in a small range. Since the ion concentration in a flame is closely related to the temperature [9], it is reasonable to set the installation location of the probes according to the aforementioned information. The position of the flame that has the maximum temperature is set to the installation location of the electrostatic probe. Observations of the flames in the experiments show that the flame length varies with the test condition. Fig. 6 shows the length of the diffusion flame at F_m = 0.80 L/min and 1.20 L/min, and that of the premixed flame at Φ = 0.54 and 3.50, respectively. The length of the inner cone for the diffusion flame under all test conditions in this study is about 55 mm and that for the premixed flame increases from 55 mm to 75 mm with Φ. In order to compare the measurement results under all test conditions, the probe was stalled 50 mm above and in parallel to the burner outlet to measure the inner cone. The length of the outer cone for the diffusion flame increases from 195 mm to 225 mm with F_m and that for the premixed flame increases from 145 mm to 180 mm with Φ. For the outer cone, it is reasonable to set the vertical distance from the probe to the burner outlet to 100 mm. Since in this case, the installation height for the diffusion flame is between 44% to 51% of the length of the outer cone and that for the premixed flame is between 56% to 69%.

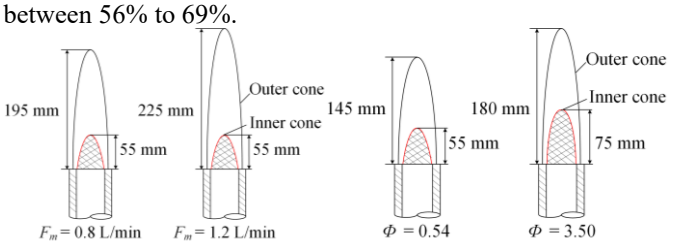

Fig. 6. Flame length under different test conditions. (a) Diffusion flame. (b) Premixed flame.

IV. RESULTS AND DISCUSSION

A. Validation of the developed electrostatic probe

Fig. 7 shows the typical signals from the electrostatic probe and the ion-current sensor for the diffusion flame at F_m = 0.90 L/min and F_m = 1.00 L/min. The signal waveforms for other fuel flowrates exhibit similar characteristics to those in Fig. 7 and hence not plotted. The DC components of the signals are removed. It is clear that either the signal from the electrostatic probe or the ion-current sensor is periodical. In addition, the electrostatic and ion-current signals have similar patterns. The amplitudes of such two signals become slightly larger as F_m increases. It can be drawn from the results that the fluctuation of the signal from the electrostatic probe arises from the variation in the density of charged species in the burner flame. The power spectral density (PSD) distributions of the electrostatic and ion-current signals, in which normalization is performed separately relative to the highest spectral peaks, are depicted in Fig. 8. It can be noticed the power spectra of the electrostatic and ion-current signals are very similar, with the same strong spectral peaks at distinct frequencies. In the signal spectra, the dominant frequencies at F_m = 0.90 L/min and F_m = 1.00 L/min are 12.8 Hz and 13.2 Hz, respectively, which agree well with the dominant frequencies of the ion-current signals. The relative values of the spectral peaks in both spectra are in good agreement. With reference to the ion-current sensor, the electrostatic probe can be employed to measure the charge density in a burner flame.

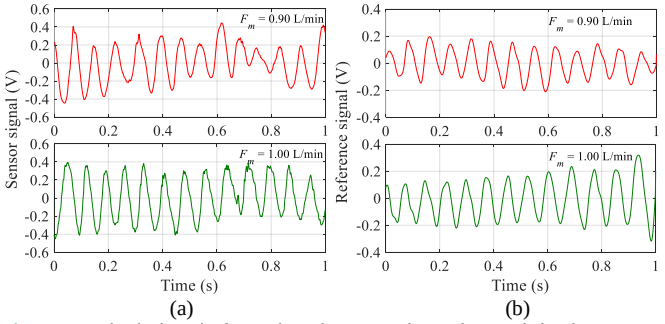

Fig. 7. Typical signals from the electrostatic probe and the ion-current sensor for the diffusion flame at F_m = 0.90 L/min and F_m = 1.00 L/min. (a) Electrostatic probe. (b) Ion-current sensor.

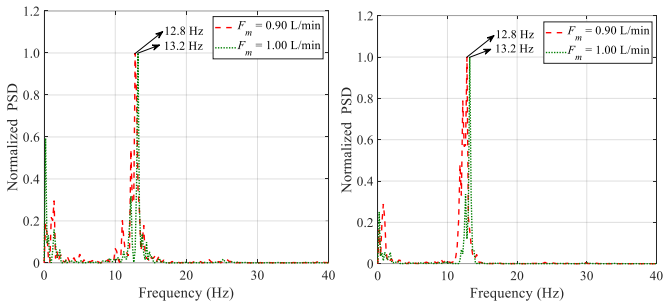

Fig. 8. Normalized power spectra of the electrostatic and ion-current signals for the diffusion flame at F_m = 0.90 L/min and F_m = 1.00 L/min. (a) Electrostatic probe. (b) Ion-current sensor.

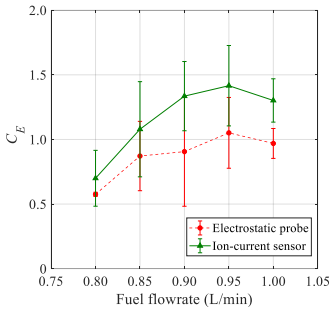

Fig. 9. Parameters for the signals from the electrostatic probe and the ion-current sensor at different fuel flowrates. (a) Peak amplitude. (b) rms value. (c) Energy.

B. Quantification of the charge density in the flame

In order to select an appropriate index to indicate the charge density in the flame, the variations in the three indexes, i.e. C_p, C_{rms} and C_E, obtained using the electrostatic probe and the ion-current sensor with the fuel flowrate, are compared. Fig. 9 compares C_p, C_{rms} and C_E of the signals from the electrostatic probe and the ion-current sensor at different fuel flowrates. Each data point is an average of 12 measurements with the standard deviation marked as an error bar. All the indexes generally follow an increasing trend with F_m. More charged soot particles at a higher F_m result in a higher average of local peak values, a larger rms value and energy of the electrostatic signal. The C_p of the electrostatic signal shows better consistency with that of the ion-current signal than the C_{rms} and C_E, and yields better repeatability with relatively smaller standard deviation mostly within 17%. The C_{rms} and C_E of the electrostatic signal generally show a similar variation trend with those of the ion-current signal, but have poor agreement and higher standard deviation mostly more than 25%. The rms value and energy of the signal, which represent the fluctuations of the signal, are used to indicate the volumetric concentration of the pneumatically conveyed particles under specific conditions [3]. However, a larger rms value or energy of the induced-charge signal for the flame, i.e. a larger fluctuation of the signal, may not represent a higher concentration of charged species in the flame. In addition, the fluctuation of the signal is higher than that of the peak amplitude, resulting in a higher standard deviation of the rms value and energy of the signal. These results show that the index, C_p, is an appropriate indicator of the charge density in the flame. A greater C_p presents a higher charge density in the flame.

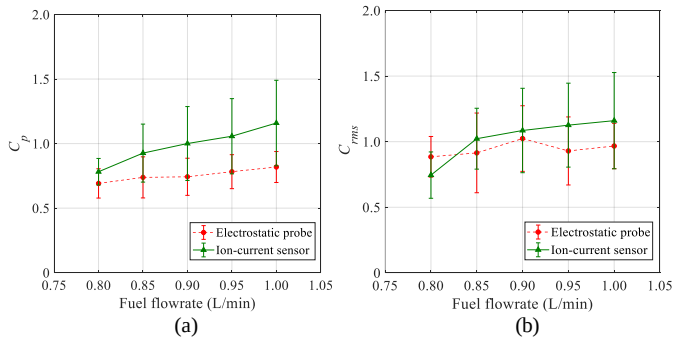

C. Experimental results

1) *Time-domain signals*

After the validation of the effectiveness of the electrostatic probe for the measurement of charge density in a burner flame, the signals from the probes for the diffusion flame at different fuel flowrates and the premixed flame at various equivalence ratios were collected. Fig. 10 shows the typical signals for the inner and outer cones of the diffusion flame at three different fuel flowrates. It can be seen in Fig. 10(a) that the signal amplitude for the inner cone increases with F_m. This is because more complicated chemical reactions in the inner cone at a higher F_m result in larger generation rate and higher concentration of charged species. The electrostatic signal for the outer cone of the diffusion flame yields a similar trend. It can be observed that the signal amplitude for the inner cone is larger than that for the outer cone. This is due to the fact that more complete combustion in the inner cone results in a larger charge density.

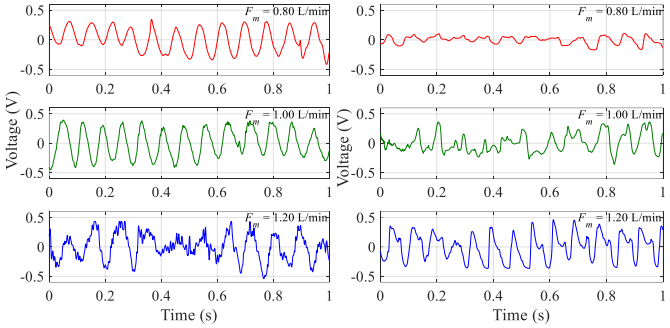

Fig. 10. Typical signals from the electrostatic probe for the diffusion flame at F_m = 0.8 L/min, 1.0 L/min, and 1.2 L/min. (a) Inner cone. (b) Outer cone.

Fig. 11 illustrates typical signals for the inner and outer cones of the premixed flame at three equivalence ratios. The electrostatic signal at $\Phi < 0.89$ is similar to that at $\Phi = 0.89$, but with a smaller amplitude. As indicated in Fig. 11(a), the signal amplitude for the inner cone at $\Phi = 1.03$ is larger as more charged species are generated due to complete combustion. In addition, noticeable higher frequency fluctuations are observed in the electrostatic signals at $\Phi = 0.89$ and $\Phi = 1.03$. This discovery is quite similar to the observation in the flame radiation signal taken at IR spectral range [21, 23]. Such results are due to the fact that the

premixed flame at $\Phi \approx 1$ is more stable in shape and exhibits more rigorous kinetic variations in the energy emission rate of reacting species [2]. It can be observed in Fig. 11(b) that the signal amplitude for the outer cone also has an increasing trend with F_m because the concentration of charged soot particles becomes larger in the fuel-rich outer cone.

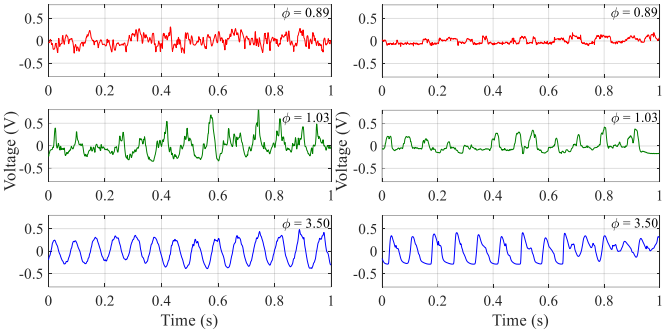

Fig. 11. Typical signals from the electrostatic probe for the premixed flame at $\Phi = 0.89$, 1.03, and 3.50. (a) Inner cone. (b) Outer cone.

2) *Spectral analyses*

Previous studies based on a noncontact electrostatic sensor array [19, 26] or the digital imaging system [21] have shown that a diffusion flame has a dominant frequency within a comparatively lower range and the frequency corresponding to the largest peak in the power spectrum is regarded as the measured oscillation frequency of the diffusion flame. A point to note is that the noncontact electrostatic sensor array or the digital imaging technique measures the fluctuations of the flame shape or brightness to characterize the flame oscillatory characteristics, whereas the developed electrostatic probe detects the variation in charge density in the flame. The power spectra of the signals from the electrostatic probe for the diffusion flame at three different fuel flowrates, are illustrated in Fig. 12. The spectra have been normalized in accordance with the maximum of the PSD values. Observations of the power spectra have shown that the diffusion flame consistently contains a single dominant frequency component. The dominant frequency at a higher F_m is slightly larger than that at a lower F_m. The measured dominant oscillation frequencies for the inner and outer cones of the diffusion flame at different fuel flowrates are depicted in Fig. 13. From Fig. 13, an increasing trend in the variations of the oscillation frequency for the inner and outer cones is evident with the increasing F_m. However, the oscillation frequency varies within a small margin, typically between 12 Hz and 14 Hz when F_m increases from 0.80 L/min to 1.20 L/min, indicating that the increasing F_m has little effect on the oscillatory characteristics of the diffusion flame.

Fig. 14 illustrates the power spectra of the signals from the electrostatic probe for the premixed flame at various equivalence ratios. In comparison with the spectra of the diffusion flame, more dominant frequencies within a wider range were observed in the spectra of the premixed flame. The oscillation frequency of a premixed flame should take the contributions of total components over the whole power spectrum into account [21, 23]. A quantitative oscillation frequency F_{pre}, is defined as the power-density-weighted average frequency over the frequency range:

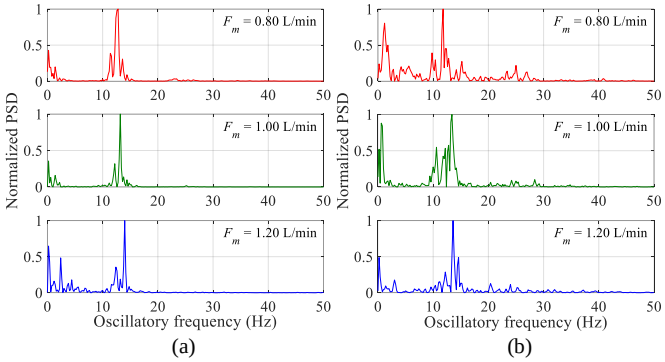

Fig. 12. Power spectra of the signals from the electrostatic probe for the diffusion flame under various fuel flowrates. (a) Inner cone. (b) Outer cone.

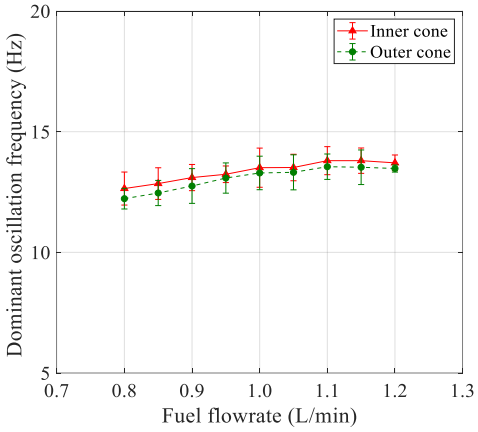

Fig. 13. Dominant oscillation frequency for the inner and outer cones of the diffusion flame for various fuel flowrates.

$$F_{pre} = \frac{\sum_{m=1}^{M}[P_{xx}(f_m) f_m]}{\sum_{m=1}^{M} P_{xx}(f_m)} \tag{8}$$

where f_m is the m-th frequency of the electrostatic signal, P_{xx} is the power density of the m-th frequency component of the signal, and M is the total number of frequency components. The weighted oscillation frequency for inner and outer cones of the premixed flame at different equivalence ratios are shown in Fig. 15. It is obvious that the oscillation frequency reaches its maximum at $\Phi = 1.03$ and then decreases with Φ. The results reveal that the flame is stable at $\Phi = 1.03$ owing to complete combustion and tends to be unstable at a higher $\Phi >$ 1.03.

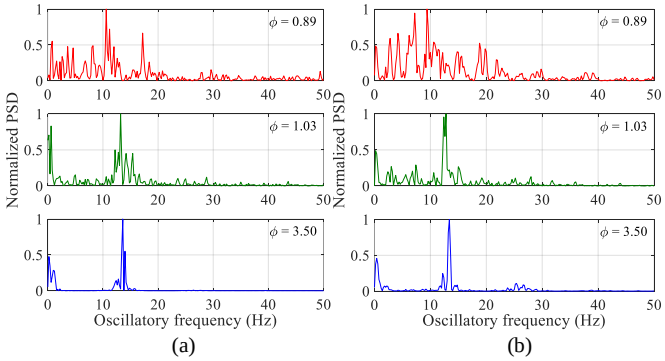

Fig. 14. Power spectra of the signals from the electrostatic probe for the premixed flame at various equivalence ratios. (a) Inner cone. (b) Outer cone.

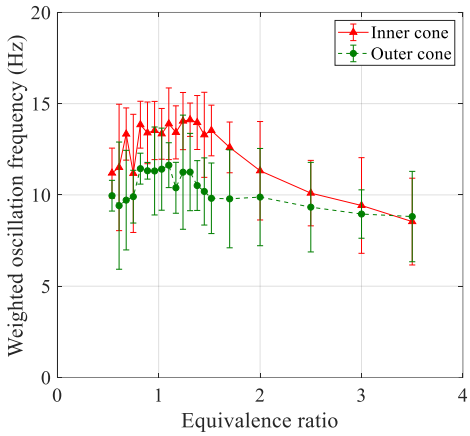

Fig. 15. Weighted oscillation frequency for the inner and outer cones of the premixed flame at various equivalence ratios.

3) *Measurement results of charge density*

The C_p of the signal from the electrostatic probe for the inner and outer cones of the diffusion flame as a function of F_m is shown in Fig. 16. It is evident that the C_p for the inner and outer cones follows an increasing trend with F_m. An explanation for this trend is that, when F_m increases, the chemi-ionization reaction rate in the blue inner cone becomes larger, resulting in the increased concentration of positive and negative ions together with electrons in the inner cone. The higher reaction rate in the yellow outer cone also brings about larger concentration of charged soot particles. For the inner cone, the C_p is larger than that for the outer cone at the same F_m. This is because the concentration of ions generated due to chemi-ionization reaction is larger than that of the charged soot particles owing to incomplete combustion. In addition, as F_m increases, the rate of increase in the C_p for the outer cone is larger than the inner cone. For a diffusion flame, the mixing of the fuel and ambient air is achieved through mass diffusion between them. The reason for aforementioned result is that the volume of ambient air is fixed, more unburned fuel diffuses outward from the center of the flame to react with the air at a higher F_m, leading to a higher reaction rate of incomplete combustion in the outer cone and hence a larger increase rate in the concentration of charged soot particles.

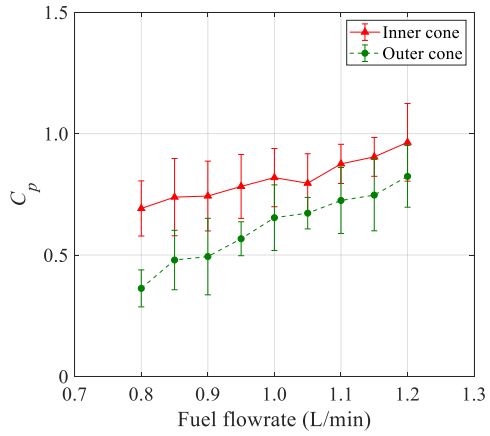

Fig. 16. Dependence of C_p for the inner and outer cones of the diffusion flame on fuel flowrate.

The C_p of the signal from the electrostatic probe for the inner and outer cones of the premixed flame as a function of equivalence ratio is illustrated in Fig. 17. The equivalence ratio ranges from 0.54 to 3.50, covering the main test conditions for typical fuel-lean, stoichiometric and fuel-rich premixed flames. The variation of the charge density in the premixed flame can be divided into three stages. The C_p of the electrostatic signal firstly yields a decreasing trend with Φ ranging from 0.54 to 0.75 in stage I, increases and reaches a local peak at Φ = 1.03 in stage II, and then continues to increase when Φ varies from 1.03 to 3.50 in stage III.

The C_p in stage I has a decreasing trend. This result is attributable to the fact that when $\Phi < 0.75$, the excess air more than required for complete combustion will reduce the temperature, resulting in incomplete combustion of part of the fuel. As Φ increases in stage I, the reduction in the amount of excess air brings about less charged soot particles produced by incomplete combustion and more ions generated from chemi-ionization reaction, leading to a reduction in the overall charge density. In stage II, when Φ is between 0.75 and 1.03, the concentration of charged soot particles continues to decrease with Φ, but the rise in the concentration of ions and electrons determines the trend of overall charge density predominantly. At Φ = 1.03, the concentration of ions and electrons reaches its maximum value because of complete combustion. The increasing trend of the C_p in stage III for the inner cone is owing to the larger concentration of positive and negative ions as well as electrons. Such an increasing trend in stage III for the outer cone is because more charged soot particles are generated due to incomplete combustion in a fuel-rich flame. It is clear from Fig. 17 that the C_p in the inner cone is consistently higher than that in the outer cone in all cases. This result can be explained by the fact a larger amount of air in the inner cone gives rise to a higher rate of chemical reaction between the unburned fuel and air, and thus a higher charge density in the inner cone.

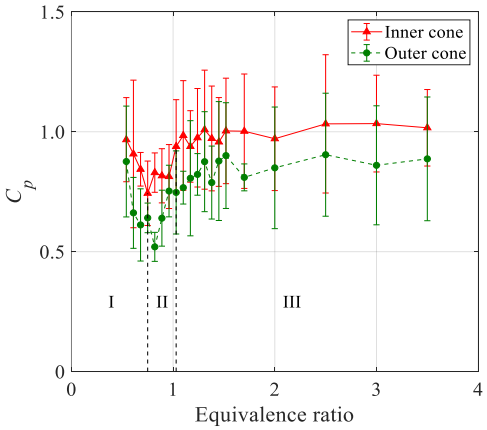

Fig. 17. Dependence of C_p for the inner and outer cones of the premixed flame on equivalence ratio.

V. Conclusions

Experimental investigations into the use of electrostatic probes for the measurement of charge density in methane fired diffusion and premixed flames have been conducted. The performance of the electrostatic probe has been validated against an ion-current sensor. Comparative studies have shown that the signals from the electrostatic probe and the ion-

current sensor have similar patterns and the relative values of the spectral peaks in both signals are in good agreement. The ratio of the dimensionless average of local peak values in the electrostatic signal to the dimensionless flame oscillation frequency, has been adopted as an indicator of the charge density, denoted by C_p. Experimental results have demonstrated that when F_m ranges from 0.8 L/min to 1.2 L/min, the charge density in the inner and outer cones of the diffusion flame follows an increasing trend. The variation of the charge density in the premixed flame can be divided into three stages when Φ ranges from 0.54 to 3.50. The charge density firstly decreases with Φ ranging from 0.54 to 0.75, then has an increasing trend and peaks when Φ = 1.03, and keeps increasing with Φ varying from 1.03 to 3.50. In addition, the charge density in the inner cone is higher than that in the outer cone for diffusion and premixed flames. Results obtained have shown that the developed electrostatic probe, together with the proposed index that combines the average of local peak values in the electrostatic signal with the flame oscillation frequency, provides a viable approach to the measurement of charge density in diffusion and premixed flames.

REFERENCES

[1] A. V. Singh, A. Eshaghi, M. Yu, A. K. Gupta and K. M. Bryden, "Simultaneous time-resolved fluctuating temperature and acoustic pressure field measurements in a premixed swirl flame," *Appl. Energy*, vol. 115, pp. 116–127, Feb. 2014.

[2] D. Sun, G. Lu, H. Zhou and Y. Yan, "Flame stability monitoring and characterization through digital imaging and spectral analysis," *Meas. Sci. Technol.*, vol. 22, no. 11, pp. 114007, Nov. 2011.

[3] Y. Yan, Y. Hu, L. Wang, X. Qian, W. Zhang, K. Reda, J. Wu and G. Zheng, "Electrostatic sensors – Their principles and applications," *Measurement*, vol. 169, pp. 108506, Feb. 2021.

[4] W. Zhao, B. Zhang, C. Xu, L. Duan and S. Wang, "Optical Sectioning Tomographic Reconstruction of Three-Dimensional Flame Temperature Distribution Using Single Light Field Camera," *IEEE Sens. J.*, vol. 18, no. 2, pp. 528–539, Jan. 2018.

[5] T. Addabbo, A. Fort, M. Mugnaini, L. Parri, V. Vignoli1, M. Allegorico, M. Ruggiero and S. Cioncolini, "Ion sensor based measurement systems: application to combustion monitoring in gas turbines," *IEEE Trans. Instrum. Meas.*, vol. 69, no. 4, pp. 1474–1483, Apr. 2020.

[6] D. Hu, Z. Cao, S. Sun, J. Sun and L. Xu, "Dual-Modality Electrical Tomography for Flame Monitoring," *IEEE Sens. J.*, vol. 18, no. 21, pp. 8847–8854, Nov. 2018.

[7] M. Balthasar, F. Mauss, and H. Wang, "A computational study of the thermal ionization of soot particles and its effect on their growth in laminar premixed flames," *Combust. Flame.*, vol. 129, no. 1–2, pp. 204–216, Apr. 2002.

[8] A. Schmidt and W. Krvll, "Electrostatic Fire Detector," *Fire Safety J.*, vol. 17, pp. 423–430, 1991.

[9] A. B. Fialkov, "Investigations on ions in flames," *Prog. Energy Combust. Sci.*, vol. 23, no. 5-6, pp. 399–528, 1997.

[10] C. S. Maclatchy and J. W. Forsman, "A novel electrostatic probe technique for measuring the ions density in a flame," *Combust. Flame.*, vol. 53, no. 1-3, pp. 41–48, Nov. 1983.

[11] T. Yokomori, S. Mochida, T. Araake and K. Maruta, "Electrostatic probe measurement in an industrial furnace for high-temperature air conditions," *Combust. Flame.*, vol. 150, no. 4, pp. 369–379, Sep. 2007.

[12] L. B. W. Peerlings, Manohar, V. N. Kornilov and P. D. Goey, "Flame ion generation rate as a measure of the flame thermo-acoustic response," *Combust. Flame.*, vol. 160, no. 11, pp. 2490–2496, Nov. 2013.

[13] F. Li, L. Xu, Z. Cao and M. Du, "A chemi-ionization processing approach for characterizing flame flicker behavior," in *Proc. IEEE Instrum. Meas. Technol. Conf.*, Pisa, ITALY, 2015, pp. 325–329.

[14] F. Li, L. Xu, M. Du, L. Yang and Z. Cao, "Ion current sensing-based lean blowout detection for a pulse combustor," *Combust. Flame.*, vol. 176, pp. 263–271, Feb. 2017.

[15] J. Guo, J. M. Goodings, A. N. Hayhurstb and S. G. Taylor, "A simple method for measuring positive ion concentrations in flames and the calibration of a nebulizer/atomizer," *Combust. Flame.*, vol. 133, no. 3, pp. 335–343, May 2013.

[16] A. N. Hayhurst, J. M. Goodings and S. G. Taylor, "The effects of applying electric fields on the mass spectrometric sampling of positive and negative ions from a flame at atmospheric pressure," *Combust. Flame.*, vol. 161, no. 12, pp. 3249–3262, Dec. 2014.

[17] H. R. N. Jones and A. N. Hayhurst, "Measurements of the concentrations of positive and negative ions along premixed fuel-rich flames of methane and oxygen," *Combust. Flame.*, vol. 166, pp. 86–97, Apr. 2016.

[18] Y. Wang, Z. Chen, Y. Li, Z. Zhou and X. Wu, "Electrical and gas-sensing properties of WO3 semiconductor material," *Solid-state Electron.*, vol. 45, no. 5, pp. 639–644, May 2001.

[19] J. Wu, Y. Yan, Y. Hu, L. Shan and W. Xu, "Flame boundary measurement using an electrostatic sensor array," *IEEE Trans. Instrum. Meas.*, vol. 70, pp. 2000412, 2021.

[20] Y. Hu, Y. Yan, L. Wang and X. Qian, "Non-Contact Vibration Monitoring of Power Transmission Belts Through Electrostatic Sensing," *IEEE Sens. J.*, vol. 16, no. 10, pp. 3541–3550, May 2016.

[21] Y. Huang, Y. Yan, G. Lu and A. Reed, "On-line flicker measurement of gaseous flames by image processing and spectral analysis," *Meas. Sci. Technol.*, vol. 10, no. 8, pp. 726–733, July 1999.

[22] A. G. Gaydon and H. G. Wolfhard, "Flames, their structure, radiation and temperature,". 4th ed. London; 1979, pp. 164–165.

[23] D. Sun, G. Lu, H. Zhou and Y. Yan, "Flame stability monitoring and characterization through digital imaging and spectral analysis," *Meas. Sci. Technol.*, vol. 22, no. 11, pp. 114007, Nov. 2011.

[24] J. Ballester and T. Garcıa-Armingol, "Diagnostic techniques for the monitoring and control of practical flames," *Prog. Energy Combust.*, vol. 36, no. 4, pp. 375–411, Aug. 2010.

[25] T. Xu and E. Hui, "Combustion," 2nd ed (in Chinese). Beijing; 2017.

[26] J. Wu, Y. Hu, Y. Yan, X. Qian and S. Gu, "Flicker measurement of burner flames through electrostatic sensing and spectral analysis," *J. of Phys., Conf. Ser.*, vol. 1065, no. 20, pp. 202004, Aug. 2018.

Yong Yan (M'04–SM'04–F'11) received the B.Eng. and M.Sc. degrees in instrumentation and control engineering from Tsinghua University, Beijing, China, in 1985 and 1988, respectively, and the Ph.D. degree in flow measurement and instrumentation from the University of Teesside, Middlesbrough, U.K., in 1992. He was an Assistant Lecturer with the Department of Automation at Tsinghua University from September 1988 to September in 1989. He joined the University of Teesside as a Research Assistant in October 1989. After a short period of postdoctoral research, he worked as a Lecturer with the University of Teesside from 1993 to 1996, and then as a Senior Lecturer, Reader, and Professor with the University of Greenwich, Chatham, U.K., from 1996 to 2004. In recognition of his contributions to pulverized fuel flow metering and burner flame imaging, he was named an IEEE Fellow in 2011 and elected as a Fellow of the Royal Academy of Engineering in 2020. He was awarded the gold medal in 2020 by the IEEE Transactions on Instrumentation and Measurement as the most published author of all time from the UK. He is currently Professor of Electronic Instrumentation and Director of Innovation at the School of Engineering, the University of Kent, Canterbury, U.K. His current research interests include multiphase flow measurement, combustion instrumentation, and intelligent measurement and condition monitoring.

Jiali Wu (S'18) received the B.Eng. degree in measurement and control technology and instrumentation from North China Electric Power University, Beijing, China, in 2016, where she is currently pursuing the Ph.D. degree in measurement technology and instrumentation. Her current research interests include flame monitoring techniques, sensor design and digital

signal processing. She is a recipient of the 2018 IEEE Graduate Fellowship Awards from the IEEE Instrumentation and Measurement Society.

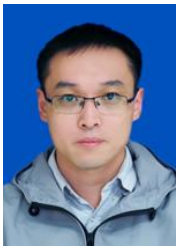

Yonghui Hu (M'11-SM'21) received the B.Eng. degree in automation from Beijing Institute of Technology, Beijing, China, in 2004, and the Ph.D. degree in dynamics and control from Peking University, Beijing, in 2009. He was a Post-Doctoral Research Fellow with Beihang University, Beijing, from 2010 to 2012, and a Research Associate with University of Kent, from 2019 to 2021. He is currently an Associate Professor with the School of Control and Computer Engineering, North China Electric Power University, Beijing. His current research interests include measurement of multiphase flow and condition monitoring of mechanical systems.